

# Guidance Law for Planar Hypersonic Descent to a Point

G. Richard Eisler\*

Sandia National Laboratories, Albuquerque,  
New Mexico 87185  
and

David G. Hull†

University of Texas at Austin, Austin, Texas 78712

## Introduction

A CONTROL law is developed for guiding a hypersonic glider in a vertical plane to a fixed point on the ground. The guidance law is based on the lift coefficient history that maximizes the final velocity. This optimal trajectory has been of interest for some time. Contensou<sup>1</sup> was the first to consider optimal control and proposed the problem for unconstrained range in terms of flight-path angle  $\gamma$  as the independent variable. This work was extended to the general problem of flight in a vertical plane,<sup>2</sup> where control solutions for all manner of constraints could be obtained by integrating a second-order, nonlinear, differential equation. However, numerical results were presented only for constrained final  $\gamma$  and altitude. No closed-form control solution exists for maximizing velocity at a fixed point. Initially, the glider is cruising at constant altitude and knows the downrange and altitude of the fixed target. Theoretically, by correct timing, the free downrange trajectory can be made to hit the target. Practically, modeling errors cause the vehicle to miss the target, but by using the neighboring optimal control, it is possible to calculate a perturbation in the optimal control, which enables the vehicle to maintain the desired downrange. Throughout this study, it is assumed that Loh's approximation<sup>3</sup> is valid, but will be updated at every sample point.

The development of the guidance rule is accomplished in two steps. First, the lift coefficient history that maximizes the final speed at a fixed final altitude, but free final downrange, is determined analytically. However, the fixed final downrange constraint is included to facilitate the derivation of the neighboring optimal control. Second, the perturbation in the lift coefficient history that enables the glider to hold the desired final downrange is derived.

To verify the guidance rule, it is flown in a three-degree-of-freedom simulation of a hypersonic glider and is shown to guide the vehicle to the target. Also, the guided trajectory is shown to compare favorably with the maximum final velocity trajectory of the simulation. Finally, some results are presented to establish the robustness of the guidance law to initial condition errors and to establish the superiority of the guidance law to that of proportional navigation.

## Optimal Control

A schematic of the guidance rule is shown in Fig. 1. At a sample point, the maximum final velocity trajectory to the ground (free final downrange) is calculated and is assumed to pass near the target. Next, the neighboring optimal path to the target (perturbed final point) is obtained, and the perturbation in the lift coefficient is added to the optimal lift coefficient

to form the desired control. This control is held constant over a sample period, and the process is repeated at the next sample point. The fixed downrange condition is included in the derivation of the free downrange optimal trajectory to facilitate the derivation of the neighboring optimal trajectory.

The equations of motion for a nonthrusting, point mass traveling in a plane over a spherical, nonrotating earth at a constant zero degree heading and at an altitude that is small with respect to the radius of the Earth are

$$\begin{aligned}\dot{x} &= V \cos \gamma, & \dot{h} &= V \sin \gamma \\ \dot{V} &= -\frac{1/2\rho V^2 S_R C_D}{m} - g_s \sin \gamma\end{aligned}\quad (1)$$

$$\dot{\gamma} = \frac{1/2\rho V^2 S_R C_L}{mV} - \left[ \frac{g_s}{V} - \frac{V}{r_s} \right] \cos \gamma$$

where  $(\cdot) = d(\cdot)/dt$ ,  $x$  is the downrange,  $h$  the altitude,  $V$  the velocity,  $\gamma$  the flight-path angle,  $\rho$  the atmospheric density,  $g_s$  the gravitational constant at the Earth's surface,  $r_s$  the Earth radius,  $S_R$  the vehicle reference area,  $m$  the vehicle mass, and  $C_L$  and  $C_D$  the lift and drag coefficients, respectively.

In the derivation of the optimal trajectory, the assumptions made are 1) flight in a great circle plane over a spherical Earth with an exponential atmosphere of scale height  $\beta$ , 2) gravitational forces are small with respect to aerodynamic forces, 3) parabolic drag polar,  $C_D = C_{D0} + KC_L^2$  with constant coefficients where  $\sqrt{C_{D0}/K} = C_L^*$  is the lift coefficient for maximum lift-to-drag ratio, and 4) Loh's approximation is valid. The equations of motion can be written in terms of nondimensional state variables  $x$  as

$$\frac{d\zeta}{d\phi} = -\frac{\cos \phi}{w(\lambda + \bar{M})}\quad (2)$$

$$\frac{dw}{d\phi} = -\frac{\sin \phi}{(\lambda + \bar{M})}\quad (3)$$

$$\frac{du}{d\phi} = \frac{1 + \lambda^2}{(\lambda + \bar{M})}\quad (4)$$

where

$$\phi = -\gamma, \quad \zeta = \frac{x}{\beta}, \quad w = \frac{\rho}{2m/(\beta S_R C_L^*)}, \quad u = \frac{C_L^*}{C_{D0}} \ln \frac{V}{\sqrt{g_s r_s}}$$

$$\lambda = \frac{C_L}{C_L^*}, \quad \bar{M} = \frac{2m \cos \gamma}{C_L^* S_R \rho r_s} \left[ 1 - \frac{g_s r_s}{V^2} \right]\quad (5)$$

Although Loh's term,  $\bar{M} < 0$ , is assumed constant over an optimal trajectory, its value is updated at each sample point.

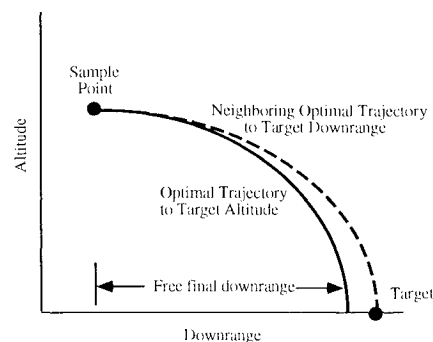


Fig. 1 Guidance schematic.

Received Oct. 3, 1991; revision received May 1, 1992; accepted for publication May 29, 1992. This paper is declared a work of the U.S. Government and is not subject to copyright protection in the United States.

\*Member of the Technical Staff, Structural Dynamics Division 1434, Associate Fellow AIAA.

†M. J. Thompson Regents Professor, Department of Aerospace Engineering, Associate Fellow AIAA.

The optimal control problem is to find the lift coefficient history,  $\lambda(\phi)$ , which maximizes the final velocity or minimizes the performance index,  $J = -u_f$ , subject to

State equations:

$$\frac{dx}{d\phi} = f(\phi, x, \lambda) \quad [\text{Eqs. (2-4)}]$$

Initial conditions:

$$\phi_o, \zeta_o, w_o, u_o \text{ known}$$

Final conditions:

$$\Psi(\phi_f, x_f) = \begin{bmatrix} \zeta_f - \zeta_{ur} \\ w_f - w_T \end{bmatrix} = 0, \phi_f \text{ free}$$

The quantity  $\zeta_{ur}$  is the nondimensional range, which results along the unconstrained or free-final range optimal path. The fixed final downrange condition is included here to facilitate the later derivation of the neighboring optimal control. From this problem statement, the Hamiltonian and the Bolza functions are constructed as

$$H = \frac{1}{(\lambda + \bar{M})} [-p_\zeta \cos \phi / w - p_w \sin \phi + p_u (1 + \lambda^2)] \quad (6)$$

$$G = -u_f + v_1(\zeta_f - \zeta_{ur}) + v_2(w_f - w_T)$$

where  $p$  and  $v$  denote Lagrange multipliers. In this section, it is assumed that the target is located at the downrange which results if no constraint is imposed on downrange. Hence,  $p_\zeta = 0$  and  $v_1 = 0$  hold.

The differential equations and boundary conditions for the  $p$  lead to  $p_\zeta = 0$ ,  $p_w = v_2$ , and  $p_u = -1$ , implying that the  $p$  are constant. Next, the optimality condition,  $H_\lambda = 0$ , combined with the Legendre condition,  $H_{\lambda\lambda} \geq 0$ , gives

$$\lambda + \bar{M} = -\sqrt{1 + \bar{M}^2 + p_w \sin \phi} \quad (7)$$

where part of the solution process has been to show that no inflection point ( $d\phi = 0$ ) can occur along the optimal path. Hence,  $\phi$  is monotonically increasing.

Finally, the natural boundary condition for  $\phi_f$  shows that  $\lambda_f = 0$ , so that from Eq. (7)

$$\sin(\phi_f) = -1/p_w \quad (8)$$

directly relating the multiplier  $|p_w| > 1$  to the trajectory.

What remains is to determine the value of  $p_w$  from the prescribed boundary conditions. Substitution of Eq. (7) into Eq. (3) and integrating gives

$$w - w_o = \sqrt{\frac{2}{b}} [-F(\Phi, k) + 2E(\Phi, k)]_{\phi_o}^{\phi_f} \quad (9)$$

where  $F$  and  $E$  are elliptic integrals of the first and second kinds, and

$$\Phi = \sin^{-1} \left[ \frac{b(1 - \sin \phi)}{a + b} \right]^{1/2}, \quad k = \left[ \frac{a + b}{2b} \right]^{1/2} \quad (10)$$

$$a = 1 + \bar{M}^2 < b = -p_w$$

Equations (8) and (9) applied at the final point can be combined into a single, nonlinear algebraic equation, which is solved by Newton's method for  $p_w$ . Once  $p_w$  is known,  $w(\phi)$  comes from Eq. (9) and  $\lambda(\phi)$  is given by Eq. (7). Finally,  $\zeta(\phi)$  and  $u(\phi)$  can be obtained from Eqs. (2) and (4), respectively, by quadrature integration (i.e., Simpson's rule) to complete the free-final-range solution.

### Neighboring Optimal Control

Assuming that the unconstrained range trajectory can be made to come close to the desired target, the process of hitting

the target can be accomplished by neighboring optimal control to a perturbed final point. The neighboring optimum formulation<sup>4</sup> is the result of linearizing the first variation conditions about the nominal optimum. It is desired to compute the optimal control and the neighboring optimal control perturbations at the sample point and hold their values constant over the sample period. If the state perturbation  $\delta x$  is zero at the sample point, the control perturbation is given by

$$\delta \lambda_o = -[H_{\lambda\lambda}^{-1} f_\lambda^T R \bar{Q}^{-1}]_{\phi_o} d\Psi_s \quad (11)$$

$d\Psi_s = [\zeta_T - \zeta_{ur} \ 0]^T$  (transpose), and is evaluated on the free-final-range optimal path. The desired perturbation in the final altitude is zero. The following relations exist along the nominal trajectory in this application:

$$n = \Psi'_f = f_f$$

$$\alpha = (G_{\phi_f} + H_f)' = p_w \cos \phi_f / \bar{M}$$

$$\bar{Q} = Q - nn^T / \alpha \quad (12)$$

$$m = (G_{\phi_f} + H_f)_{x_f} = 0$$

$$\bar{R} = R - mn^T / \alpha = R$$

where the notation  $(\cdot)_{\phi_f}$ ,  $(\cdot)_{x_f}$ ,  $(\cdot)' = \partial(\cdot)/\partial\phi_f$ ,  $\partial(\cdot)/\partial x_f$ ,  $d(\cdot)/d\phi_f$ , respectively. The quantities  $H_{\lambda\lambda}$  and  $f_\lambda$  are given by

$$H_{\lambda\lambda} = -\frac{2}{\lambda + \bar{M}}, \quad f_\lambda = \frac{1}{(\lambda + \bar{M})^2} \begin{bmatrix} \cos \phi / w \\ \sin \phi \\ p_w \sin \phi \end{bmatrix} \quad (13)$$

where  $\lambda + \bar{M}$  is given by Eq. (7).  $R$  can be calculated by integrating

$$\frac{dR}{d\phi} = -f_\lambda^T R = \frac{1}{\lambda + \bar{M}} \begin{bmatrix} 0 & 0 \\ -\cos \phi / w^2 & 0 \\ 0 & 0 \end{bmatrix} \quad (14)$$

where

$$R(\phi_f) = \left[ \frac{\partial \Psi}{\partial x} \right]_{\phi_f}^T = \begin{bmatrix} 1 & 0 \\ R_{21} & 1 \\ 0 & 0 \end{bmatrix}_{\phi_f} = \begin{bmatrix} 1 & 0 \\ 0 & 1 \\ 0 & 0 \end{bmatrix} \quad (15)$$

Then, with  $R(\phi)$  known,  $\bar{Q}$  can be obtained from

$$\frac{d\bar{Q}}{d\phi} = -R^T f_\lambda^T H_{\lambda\lambda}^{-1} f_\lambda R = -\frac{1}{2(\lambda + \bar{M})^3} \begin{bmatrix} a_1^2 & a_1 a_2 \\ a_1 a_2 & a_2^2 \end{bmatrix}, \quad \bar{Q}_f = 0 \quad (16)$$

where  $a_1 = R_{21} \sin \phi + \cos \phi / w$ ,  $a_2 = \sin \phi$ . In order to prove the feasibility of this method, a Runge-Kutta scheme was used to integrate the  $R$  and  $\bar{Q}$  equations; however, a quadrature scheme could be used to gain execution speed due to the uncoupled  $R$  equation. Note that only one element of  $R$  is needed for the computation of  $\bar{Q}$ . Finally,  $\bar{Q}$  is formed as  $\bar{Q} = Q - nn^T / \alpha$ , where  $n$  and  $\alpha$  are given in Eq. (12).

### Guidance Law

The guidance law or the feedback control law to achieve  $\zeta_T$  and  $w_T$  for a given value of  $\bar{M}$  is the sum of  $\lambda$  in Eq. (7) and  $\delta \lambda_o$  in Eq. (11), or

$$\lambda_o = -\sqrt{1 + \bar{M}^2 + p_w \sin \phi_o} - \bar{M} + \frac{(R_{21} \sin \phi_o - \cos \phi_o / w_o)(\bar{Q}^{-1})_{22} - \sin \phi_o (\bar{Q}^{-1})_{21}}{2|\bar{Q}^{-1}| \sqrt{1 + \bar{M}^2 + p_w \sin \phi_o}} (\zeta_T - \zeta_{ur}) \quad (17)$$

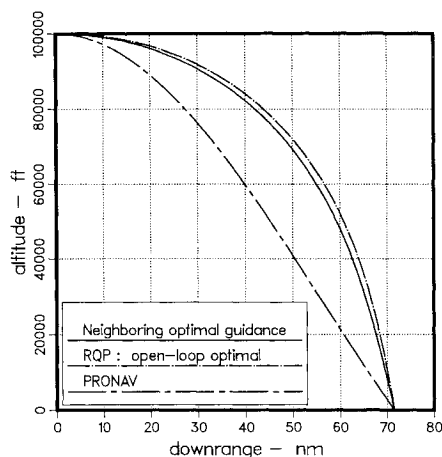


Fig. 2 Altitude downrange comparisons.

At each sample point, the value of  $\bar{M}$  is updated from inertial measurements.

To demonstrate the effectiveness of this guidance law, it has been flown in a three-degree-of-freedom simulation containing a true time-based physical flight model, a standard atmosphere, and wind-tunnel based aerodynamics.<sup>5</sup> Results are shown in Fig. 2 for a sample time of  $\Delta t = 0.1$  s.

Also shown in these figures are the open-loop optimal trajectory for the simulation model and the trajectory obtained from proportional navigation (PRONAV). The open-loop optimal trajectory has been obtained for a piecewise-linear control (suboptimal control) using recursive quadratic programming (RQP).<sup>6</sup> The PRONAV guidance law is that of the linear-quadratic control law of Ref. 7. Weighting is for miss distance only, leading to the familiar control gain,  $K = 3/t_{go}^2$ , where  $t_{go}$  is calculated at each sample point as (range/range rate).

A fourth-order, fixed step, Runge-Kutta integrator is used in all simulations. The nominal trajectory boundary conditions (initial-final) for the example problem are:  $\gamma = 0$  degree,  $x = 0$  nm-71.51 (the final downrange is that predicted by the proposed guidance scheme at the initial value of  $\bar{M}$ ),  $h = 100,000$  ft-0,  $V = 11,000$  ft/s-max.

Figure 2 displays the simulation flight profiles. The neighboring optimal guidance and RQP have the same general glide-and-dive contour, vs PRONAV, which turns quickly to line up with the target. These first two simulations shift the majority of flight time to the higher altitudes, where drag is low.

The true optimal velocity produced by the RQP scheme is 7090 ft/s for a flight time of 45 s. The terminal velocity generated by the proposed method differs from it by less than 1%, whereas the PRONAV solution is about 40% less, with a 10% increase in flight time. Because they take advantage of the atmospheric density variation during descent, lift coefficient variation is moderate for the optimal scheme, vs PRONAV, which applies maximum turning from the start to line up with the target.

The issue of robustness was addressed by examining the ability to hit the nominal target (i.e., 71.51 nm downrange) given changes in initial velocity and downrange. Velocity perturbations of  $\pm 2000$  ft/s and downrange perturbations of  $\pm 10$  nm were used. In each case, the vehicle was able to hit the target. For a given initial velocity, terminal velocity results appear relatively insensitive to initial downrange perturbations.

### Conclusions

A sampled-data feedback control method has been devised to obtain approximate, maximum-terminal-velocity descent trajectories in a vertical plane at a designated target. These trajectories are characterized by glide-and-dive flight to the target to minimize the time spent in the denser parts of the

atmosphere. The proposed on-line scheme uses neighboring optimal theory to successfully bring final altitude and range constraints together, as well as compensate for differences in flight model, atmosphere, and aerodynamics. Comparison with the open-loop optimal trajectory for the terminal velocity is excellent and far exceeds the proportional navigation solution. The scheme also demonstrates robustness to significant perturbations in initial velocity and downrange.

### Acknowledgment

This work was performed at Sandia National Laboratories supported by the U.S. Department of Energy under Contract DE-AC04-76DP00789.

### References

- Contensou, P., "Contribution à l'Etude Schematique des Trajectories Semi-Balistique à Grand Portee," Communication to Association Technique Maritime et Aeronautique, Paris, 1965.
- Busemann, A., Vinh, N. X., and Kelley, G. F., "Optimum Maneuvers of a Skip Vehicle with Bounded Lift Constraints," *Journal of Optimization Theory and Applications*, Vol. 3, No. 4, 1969, pp. 243-262.
- Loh, W. H. T., *Dynamics and Thermodynamics of Planetary Entry*, Prentice-Hall, Englewood Cliffs, NJ, 1963.
- Bryson, A. E., and Ho, Y. C., *Applied Optimal Control*, Halstead, New York, 1975.
- Eisler, G. R., and Hull, D. G., "Optimal Descending, Hypersonic Turn-to-Heading," *Journal of Guidance, Control, and Dynamics*, Vol. 10, No. 3, 1987, pp. 255-261.
- Powell, M. J. D., "A Fast Algorithm for Nonlinearly Constrained Optimization Calculations," *Proceedings of the Biennial Conference on Numerical Analysis, 28 June-1 July 1977*, edited by G. A. Watson, Springer-Verlag, Berlin, Germany, 1978, pp. 144-157.
- Riggs, T. L., and Vergez, P. L., "Advanced Air-to-Air Missile Guidance Using Optimal Control and Estimation," Air Force Armament Laboratory, TR-81-56, Eglin Air Force Base, Florida, June 1981.

## Factorization Approach to Control System Synthesis

A. Nassirharand\*

Scientific Institute of Scholars, Reno, Nevada 89501

### Nomenclature

- $a(s) = a(s) \in \Psi$   
 $b(s) = b(s) \in \Psi$   
 $D(s) = D(s) \in H$ ; the pair  $[N(s), D(s)] \in H$  are coprime factors of  $h_{y,u}^p$   
 $H$  = commutative algebraic ring;  $H \subset R(s)$  with Hurwitz denominator polynomials  
 $h$  = altitude; 30,000 ft  
 $h_{y,u}$  = closed-loop input-output map  
 $h_{y,u}^p$  = desired closed-loop input-output map  
 $h_{y,u}^p$  = plant input-output map  
 $M$  = Mach number; 0.84  
 $m(s) = m(s) \in \Psi'$   
 $N(s) = N(s) \in H$ ; see  $D(s)$   
 $n_r$  = number of unknown coefficients on the right-hand side of the Bezout identity  
 $P(s) = P(s) \in H$ ; the pair  $[P(s), Q(s)] \in H$  is coprime and satisfies the Bezout identity

Received April 23, 1991; revision received Nov. 24, 1991; accepted for publication Feb. 4, 1992. This paper is declared a work of the U.S. Government and is not subject to copyright protection in the United States.

\*President and Director, P.O. Box 3095. Member AIAA.